Regenerative Therapy 28 (2025) 358–370

Contents lists available at ScienceDirect

Regenerative Therapy

journal homepage: http://www.elsevier.com/locate/reth

Original Article

Quercetin prevents the loss of chondrogenic capacity in expansion cultured human auricular chondrocytes by alleviating mitochondrial dysfunction

Hua Tong [a, b, 1], Xudong Guo [d, 1], Lili Chen [a, b], Honglei Wang [a, b], Xuerui Hu [a, b], Aijuan He [a, b], Chenlong Li [a, b], Tianyu Zhang [a, b, c, *], Jiuhong Kang [d, **], Yaoyao Fu [a, b, ***]

[a] Department of Facial Plastic and Reconstructive Surgery, Eye & ENT Hospital, Fudan University, Shanghai 200031, China
[b] ENT Institute, Eye & ENT Hospital, Fudan University, Shanghai 200031, China
[c] NHC Key Laboratory of Hearing Medicine, Fudan University, Shanghai 200031, China
[d] School of Life Sciences and Technology, Tongji University, Shanghai 200092, China

ARTICLE INFO

Article history:
Received 10 November 2024
Received in revised form
25 December 2024
Accepted 4 January 2025

Keywords:
Tissue engineering
Chondrocytes
Senescence
Mitochondrial dysfunction
Quercetin

ABSTRACT

Objective: To explore the characteristics of cellular senescence in human auricular chondrocytes during long-term in vitro culture and to evaluate the effects of anti-senescence treatments on enhancing their chondrogenic function.

Methods: Auricular chondrocytes exhibited senescence-related characteristics after prolonged expansion in culture. To identify senescence inducers, transcriptome sequencing was performed, with findings corroborated by transmission electron microscopy analyses. Quercetin was employed as an intervention to mitigate cellular senescence progression. The alterations in cellular senescence and mitochondrial function were evaluated. Regenerative cartilage tissue was developed through in vitro chondrogenic induction and in vivo implantation with GelMA hydrogel-loaded cells in nude mice. The impact of quercetin was substantiated through histological examinations.

Results: Mitochondrial dysfunction was a key characteristic of auricular chondrocytes after long-term expansion culture. Chondrocytes cultured with quercetin showed a lower proportion of senescent cells and reduced mitochondrial dysfunction. The chondrocytes cultured with continuous application of quercetin formed higher quality regenerative cartilage both in vitro and in vivo compared to the control group.

Conclusion: The results reveal that quercetin attenuates chondrocyte senescence by alleviating mitochondrial dysfunction, thereby preventing the loss of chondrogenic function in chondrocytes subjected to long-term expansion culture.

1. Introduction

Cartilage is a type of connective tissue composed of chondrocytes and abundant extracellular matrix. Tissue-engineered cartilage transplantation is a novel clinical technique developed to address cartilage defect diseases [1]. This approach involves the in vitro expansion of autologous chondrocytes, which are then seeded onto a three-dimensional scaffold material and cultured with growth factors to construct pre-shaped regenerative cartilage before being transplanted into the site of cartilage defects in vivo to

* Corresponding author. Department of Facial Plastic and Reconstructive Surgery, ENT institute, Eye & ENT Hospital, NHC Key Laboratory of Hearing Medicine (Fudan University), Shanghai 200031, China.
** Corresponding author.
*** Corresponding author. Department of Facial Plastic and Reconstructive Surgery, ENT institute, Eye & ENT Hospital, Shanghai 200031, China.
E-mail addresses: tyzhangent2006@163.com (T. Zhang), jhkang@tongji.edu.cn (J. Kang), fuyaoyao2007@126.com (Y. Fu).
Peer review under responsibility of the Japanese Society for Regenerative Medicine.
[1] These authors contributed equally to this work.

https://doi.org/10.1016/j.reth.2025.01.005

achieve repair [2–4]. The scaffold material loaded with cells gradually degrades after transplantation, so the mechanical properties of the regenerative cartilage largely depend on the chondrocytes' ability to secrete extracellular matrix components like glycoproteins, proteoglycans, and chondroitin sulfate. If the chondrocytes have a weakened ability to produce extracellular matrix, the tissue-engineered cartilage cannot achieve sufficient mechanical strength, leading to graft deformation and resorption [5].

To obtain a sufficient number of chondrocytes for transplantation, in vitro expansion of cells is essential. However, during the expansion period, chondrocytes rapidly lose their ability to secrete normal cartilage extracellular matrix components and develop an abnormal extracellular matrix secretion phenotype, ultimately converting into irreversibly myofibroblast-like cells [6,7]. How to effectively maintain the normal secretion function while expanding chondrocyte numbers remains a critical challenge [8–10].

Our recent study has found that human auricular chondrocytes comprise multiple subpopulations at different developmental stages, including chondrogenic stem/progenitor cells with high proliferative potential and mature chondrocytes with low proliferative potential and prone to senescence [11]. Regardless of the differentiation maturity of chondrocytes, senescence is inevitable during in vitro culture. Senescent chondrocytes not only exhibit a loss of function in secreting cartilage extracellular matrix [12], but also adversely affect chondroprogenitor cells in a shared culture environment by paracrine release of inflammatory factors (senescence-associated secretory phenotype), such as inhibiting proliferation, inducing abnormal differentiation, and promoting senescence. Therefore, the effects and mechanisms of inhibiting cellular senescence in improving the chondrogenic function of chondrocytes in long-term in vitro culture may far exceed our previous understanding [13].

For tissue-engineered cartilage ear reconstruction surgery, autologous auricular cartilage is currently the optimal source of seed cells [14,15]. In patients with congenital microtia, the deformed auricle contains incompletely developed auricular cartilage, which need complete removal in ear reconstruction surgery. Harvesting these discarded cartilage tissues is safe and convenient, without damaging normal physiological functions, thus serving as an excellent source for constructing tissue-engineered cartilage [2]. Consequently, we aimed to explore whether interventions to inhibit cellular senescence could mitigate the loss of chondrogenic capacity in auricular chondrocytes from patients with microtia during long-term in vitro culture.

In this study, we first conducted comparative analyses on chondrocytes from different passage numbers (zero and five passages). Various methods such as cell morphology observation, phenotypic gene expression levels, and senescence-associated β-galactosidase staining were employed to observe senescence characteristics in passage cultured chondrocytes. Additionally, transcriptome sequencing was used to analyze gene expression in chondrocytes, revealing that senescent auricular chondrocytes exhibit enrichment in biological processes such as oxidative stress, tissue remodeling, DNA repair, and mitochondrial membrane dysfunction. Based on these findings, we selected quercetin, a natural flavonoid compound, which reduces senescence in auricular chondrocytes during passaging expansion culture. The results showed that quercetin prevents the loss of chondrogenic capacity of chondrocytes after long-term in vitro culture. Overall, this study demonstrates that anti-senescence measure during in vitro culture is effective in preventing the loss of function in auricular chondrocytes and provides new perspective and strategy to improve the quality of tissue-engineered auricular cartilage construction.

2. Materials and methods

2.1. Cell culture

With approval from our hospital's ethics committee, samples were sourced from auricular cartilage discarded during auricular reconstruction surgery in patients with third-degree congenital microtia, aged 8–12, all of whom provided informed consent. The auricular cartilage samples were immediately washed with sterile saline to remove surface blood and carefully dissected to remove the soft tissue from the cartilage surface. The cartilage was stored on ice and transported to the laboratory. Cartilage tissues were cut into 2–3 mm^3 pieces using ophthalmic scissors and blades, washed three times with PBS, and then transferred into a 50 mL centrifuge tube containing 0.15 % type II collagenase (ST2303, Beyotime) prepared in DMEM (11960044, Gibco), filtered through a 0.22 μm bacterial filter. The tube was sealed and placed in a 37 °C shaking incubator for digestion at 100 rpm. Cartilage samples from different patients were digested separately, and after 18 h, the cell suspension was filtered through a 40 μm strainer. Cells were collected by centrifuging at 300×*g* for 5 min, washed again with PBS twice, and resuspended. The cell suspension was aliquoted into cryopreservation media and stored in liquid nitrogen. The culture medium consisted of DMEM, 10 % FBS (A5256701, Gibco), and 1 % penicillin-streptomycin (10378016, Gibco). Cells were seeded at a density of 1×10^4 cells/cm^2, incubated at 37 °C with 5 % CO_2, with medium changes every 2 days. Cells displaying normal growth under a microscope were selected for further passaging after 5–7 days.

Anti-senescence intervention begins in auricular chondrocytes that have been passaged in vitro twice(CC-P2). Starting from the second day after seeding, quercetin (HY-18085, MCE), with DMSO (D2650, Sigma) as the vehicle, is added to the cell culture medium, with the medium being changed every 2 days thereafter. The control group consisted of auricular chondrocytes with the same concentration of DMSO added but without quercetin, with all other culture conditions and passage times being the same.

2.2. Immunofluorescence staining

Chondrocytes were seeded on the surface of a sterile circular glass slide with a diameter of 14 mm and cultured for 5 days. The slides were then placed on ice, washed with pre-cooled PBS, and fixed with pre-cooled 4 % PFA for 10 min. Following three PBS washes, 0.2 % Triton X-100 was added for 15 min for permeabilization, followed by blocking with 5 % donkey serum for 30 min. The surface liquid was removed, and primary antibodies [rabbit anti-human COL2A1 (AF5456, Abcam), dilution 1:200; rabbit anti-human γH2AX (AP0687, Abclonal), dilution 1:2000] diluted in 1 % BSA were applied and incubated overnight at 4 °C. After three PBS washes, secondary antibody [goat anti-rabbit CoraLite488 (SA00013-2, Proteintech), dilution 1:300] was applied and incubated in the dark at room temperature for 2 h. Following three PBS washes, Rhodamine Phalloidin (RM02835, Abclonal) was added and incubated in the dark at room temperature for 20 min. After three PBS washes, DAPI (CM07245, Proteintech) was applied for 10 min at room temperature in the dark. Finally, after three PBS washes, an anti-fluorescence mountant was applied to preserve the slides for observation under a confocal microscope (SP8, Leica).

2.3. Real-time quantitative PCR

For each sample, one million cells were collected and lysed using RNAiso (9108, TaKaRa), followed by total RNA extraction with the TRIzol method. Reverse transcription was conducted in a 10 μl

system (37 °C for 15 min; 85 °C for 5 s), and the cDNA obtained was stored at −80 °C for later use. Real-time PCR reactions were performed in a 10 μl system (95 °C for 15 s; 95 °C for 15 s, 40 cycles; 60 °C for 30 s), using GAPDH as the reference gene. The relative expression levels of target genes were calculated by the $2^{-\Delta\Delta Ct}$. Primer sequences are listed in Table 1.

2.4. SA-β-gal staining

Remove the culture medium from the 6-well plates and wash with PBS once. Add 1 mL of 4 % PFA to each well and fix at room temperature for 15 min. After removing the PFA, wash cells three times with PBS, each for 3 min. Prepare the SA-β-gal staining solution (C0602, Beyotime) according to the kit instructions, mixing solutions A, B, C, and X-Gal in a 10:10:930:50 ratio. Add 1 mL of the staining working solution to each well, seal the 6-well plate with parafilm to prevent evaporation, and incubate overnight at 37 °C. Remove the staining solution and replace it with PBS. Observe the staining results using an inverted phase-contrast microscope.

2.5. EdU detection

Dilute EdU stock solution (C0071S, Beyotime) in DMEM at a 1:500 ratio to prepare a 20 μM working solution. On the third day of cultivation, add pre-warmed EdU working solution with an equal volume of culture medium to the 6-well plates. Cells without EdU were used as negative controls. After 3 h, remove the medium and wash with PBS once, then add 1 mL of 0.25 % trypsin to each well for 3-min digestion. Collect cells into 1.5 mL EP tubes, centrifuge at 300×*g* for 3 min, and resuspend in PBS. Centrifuge again at 300×*g* for 3 min, resuspend in 1 mL of 4 % PFA with gentle pipetting, and fix at room temperature for 15 min. Wash cells three times with PBS. Add 1 mL of permeabilization solution containing 0.3 % Triton X-100, incubate at room temperature for 10 min, and wash cells twice with PBS. Use Edu staining kit protocol to prepare the Click reaction working solution in a 430:20:1:50 ratio with Click Reaction Buffer, CuSO4, Azide 488, and Click Additive Solution. Add 0.5 mL of this solution to each tube, gently pipette the cells, and incubate for 30 min in the dark at room temperature. Wash with PBS three times then proceed with flow cytometry (FACSVerse, BD) to collect FITC channel fluorescence signals.

2.6. Transcriptome sequencing

Extract total RNA from cells and assess RNA integrity using the Agilent 2100 bioanalyzer. Enrich mRNA using the Oligo(dT) magnetic bead method. Fragment the mRNA randomly and construct the library. Quantify the library accurately to ensure an effective concentration greater than 1.5 nM. Perform library amplification with dNTPs labeled with four fluorescent tags, DNA polymerase, and adapter primers. Capture fluorescence signals with the sequencer, filter raw sequencing data, and ensure sequencing error rates and GC content distribution meet quality checks to obtain clean reads. Align clean reads to the human reference genome using HISAT2 for gene annotation, and count reads per gene using Subread to generate expression matrices for all samples. Biological replicates were processed using DESeq2 for differential gene screening, followed by gene enrichment analyses using GO, KEGG, Reactome, DO, DisGeNET, GSEA, and protein interaction networks.

Table 1
Primers used in this study.

Genes	Forward(5′-3′)	Reverse(5′-3′)
COL2A1	TGGACGATCAGGCGAAACC	GCTGCGGATGCTCTCAATCT
ACAN	GCCTGCGCTCCAATGACT	ATGGAACACGATGCCTTTCAC
COL1A1	TGACGAGACCAAGAACTGCC	GGTCGGTGGGTGACTCTGA
COL3A1	TTGAAGGAGGATGTTCCCATCT	ACAGACACATATTTGGCATGGTT
CDKN1A	TGTCCGTCAGAACCCATGC	AAAGTCGAAGTTCCATCGCTC
GAPDH	CTCAAGATCATCAGCAATGCCT	ACAGTCTTCTGGGTGGCAGT

2.7. Transmission electron microscopy

Select cells for detection, remove the culture medium, and immediately add 2.5 % glutaraldehyde. Use a cell scraper to gently collect all cells into a 15 mL centrifuge tube. Centrifuge at 300×*g* for 3 min, add fresh 2.5 % glutaraldehyde, fix at room temperature for 2 h, and then transfer to a 4 °C refrigerator overnight. Wash three times with PBS (pH 7.4), each for 15 min. Add 1 % osmium acid to fix at room temperature (20 °C) for 2 h. Wash with PBS (pH 7.4) three times, each for 15 min. Dehydrate gradually in 50 %, 70 %, 80 %, 90 %, 95 %, 100 %, and 100 % ethanol for 15 min each step. Infiltrate cell pellets with a 1:1 mixture of acetone and 812 embedding resin overnight. Pour pure 812 resin into embedding molds, insert cell samples, and polymerize at 60 °C for 48 h. Prepare ultra-thin 60–80 nm sections, stain doubly with uranyl acetate and lead citrate for 15 min each, and dry sections overnight at room temperature. Observe and collect images using a transmission electron microscope (GEMIN300, ZEISS).

2.8. CCK-8 assay

Seed chondrocytes into 96-well plates at 2000 cells per well (100 μL per well). Begin treatment one day after seeding with media containing different concentrations of quercetin, refreshing the media every two days. Conduct CCK-8 analysis on days 1, 3, 5, and 7. Add 10 μL of CCK-8 solution (C0042, Beyotime) per well and set up blank controls without cells. Incubate in a cell culture incubator for 1 h, then read absorbance at 450 nm using a microplate reader (SpectraMax iD3, MolecularDevices). Record OD values for statistical analysis.

2.9. JC-1 assay

Dilute JC-1 stock solution (abs50016, Absin) by adding 50 μL JC-1 (200 ×) to 8 mL ultrapure water, shake to dissolve completely, then add 2 mL JC-1 staining buffer (5 ×) to make JC-1 staining working solution (1 ×). Remove culture media from 6-well plates and add 0.5 mL fresh culture medium with 10 % serum, followed by an equal volume of JC-1 staining solution (1 ×), incubate at 37 °C for 20 min. Prepare JC-1 staining buffer (1 ×) by mixing JC-1 staining buffer (5 ×) with ultrapure water in a 1:1 ratio and store on ice for later use. After incubation, wash cells twice with JC-1 staining buffer (1 ×). Finally, observe and capture images under a fluorescence microscope.

2.10. MitoSOX assay

Dilute MitoSOX Red (S0061S, Beyotime) to working concentration by mixing 1 μl MitoSOX Red (5 mM) with 1 mL PBS. Resuspend cells in PBS after trypsin digestion and cell counting, centrifuge at 600×*g* for 5 min at room temperature. Discard the supernatant and resuspend cells in 0.5 mL MitoSOX Red staining solution in each tube. Incubate at 37 °C in a cell incubator for 20 min, then centrifuge at 600×*g* for 3 min at 4 °C, wash twice with PBS. Finally, analyze with flow cytometry, collecting PE channel fluorescence signals.

2.11. Proteomics analysis

Digest and collect cells, count them, lyse with RIPA buffer (P0013B, Beyotime), and centrifuge at 12,000×*g* for 20 min at 4 °C. Quantify the supernatant protein with BCA (P0010S, Beyotime), sending 100 μg protein per sample for analysis. Digest protein samples into peptides, separate by liquid chromatography, and test with mass spectrometry. Compare the ion peaks with human protein sequences from the Uniprot database for protein identification and quantification. Transform gene expression data by log2(x+1), calculate p-values, and identify differentially expressed genes with Fold change >1.5 and p-value <0.05, using a heatmap to reflect results. Mark significantly upregulated proteins in red and downregulated proteins in blue. Use the R package clusterProfiler for differential protein enrichment analysis, employing the enrichGO function for over-representation analysis, focusing on the GOBP (Gene Ontology Biological Process) annotation database, with a p-value threshold of 0.05 and FDR for multiple testing. Compile a comprehensive list of mitochondrial-related nuclear genes from MitoCarta3.0, Acumenta Biotech, MitoMiner 4.0, and MitoProteome. After removing duplicates, obtain a set of 2622 genes related to mitochondrial function. Intersect these genes with differentially expressed genes from proteomics to produce a volcano plot. Subsequently, conduct GO functional enrichment and Gene Set Variation Analysis (GSVA) for mitochondrial-related differentially expressed genes.

2.12. SPiDER-βGal staining

Digest with 0.25 % trypsin and collect cells, adding 5×10^5 cells per sample into a 1.5 mL EP tube. After centrifuging at 300×*g* for 3 min, remove the digestive solution. Add 1 mL of 4 % PFA solution to each tube and fix at room temperature for 3 min. Resuspend the cells with Hanks' HEPES buffer and wash the cells twice using the same procedure. Dilute SPiDER-βGal (SG02, Dojindo) to the working concentration using McIlvaine buffer (pH 6.0). Add 0.5 mL of the SPiDER-βGal working solution to each EP tube and incubate at 37 °C for 15 min. Wash and resuspend the cells once with Hanks' HEPES buffer. Analyze cell fluorescence using a flow cytometer (488 nm excitation, collect FITC fluorescence signal).

2.13. Cartilage tissue culture

Chondrogenic induction in vitro was performed using auricular chondrocytes after five passages(CC-P5). Prepare chondrogenic induction medium by supplementing DMEM with 10 ng/mL TGF-β1 (RP01458, ABclonal), 100 ng/mL IGF-1 (RP00996, ABclonal), 1 % ITS (AR013, R&D), 40 ng/mL dexamethasone (D4902, Sigma), 50 μg/mL vitamin C (A5960, Sigma), and 1 % penicillin and streptomycin. Centrifuge collected CC-P5 at 300×*g* for 3 min, resuspend in chondrogenic induction medium, and transfer 2×10^5 cells/mL suspension into each 15 mL centrifuge tube, centrifuge at 300×*g* for 5 min. Place the loosely capped tube upright in the incubator. Change to fresh chondrogenic medium the next day, and continue changing the chondrogenic induction medium every two days. After 21 days, collect cartilage for observation, dehydration, embedding, sectioning, and staining.

2.14. Subcutaneous transplantation in mice

BALB/c nude mice (6-week-old, male) were procured from Shanghai GemPharmatech. All experimental protocols were approved by the Ethics Committee of the Eye & ENT Hospital, Fudan University. The mice were anesthetized using inhalation of sevoflurane. CC-P5 cells were resuspended in sterile gelatin methacryloyl (GelMA) hydrogel, adjusting the concentration to 50 million cells/mL. A volume of 0.2 mL of the cell-laden hydrogel was injected subcutaneously into the mice. For both the control and quercetin-treated groups, CC-P5 was symmetrically injected on both sides of the backs of the mice at subcutaneous sites. Identification was achieved using ear studs. After 5 weeks, the subcutaneous cartilage formed was retrieved for dehydration, embedding, sectioning, and staining analysis.

2.15. Statistical analysis

Statistical analysis was performed using Prism 9 software (GraphPad Software). Quantitative results are expressed as the mean ± standard error of the mean (SEM). Comparisons between two groups were conducted using a two-tailed Student's t-test. For multiple group comparisons, one-way ANOVA followed by Tukey's post hoc multiple comparisons test was used. A p-value of less than 0.05 was considered statistically significant. Data were derived from at least three biological replicates, with experiments repeated more than twice.

3. Results

3.1. The senescence of auricular chondrocytes is exacerbated after long-term culture

We first utilized immunofluorescence staining to observe changes in auricular chondrocytes following long-term culture. The findings indicated that the primary cultured chondrocytes (CC—P0) exhibited a polygonal morphology with pseudopodial structures at the cell edges, and the cytoplasm showed widespread expression of COL2A1. Filamentous actin (F-actin) mainly localized at the cytoplasmic periphery and within the pseudopodia. In contrast, CC-P5 exhibited weakened expression of COL2A1, and their intracellular F-actin became dense and thickened (Fig. 1-a). The matrix secretion function of chondrocytes was assessed using qPCR, showing that the expression levels of chondrogenic genes COL2A1 and ACAN in CC-P5 were significantly lower than in CC-P0 (Fig. 1-b). Meanwhile, genes indicative of fibrotic levels, such as COL1A1 and COL3A1, were expressed more in CC-P5 than in CC-P0 (Fig. 1-c). These results suggest that chondrocytes exhibit a diminished chondrogenic phenotype and an enhanced fibrotic phenotype after long-term culture. This phenotypic shift indicates the transdifferentiation of chondrocytes into a pathological cell type resembling myofibroblasts.

To determine the changes in the degree of senescence during the aforementioned phenotypic transition, we employed the senescence-associated β-galactosidase (SA-β-gal) staining to assess the proportion of senescent cells. Under a light microscope, CC-P0 appeared morphologically homogeneous and spindle-shaped, and only a small proportion of cells stained blue can be observed. Conversely, CC-P5 had a larger spread area and exhibited a more pronounced morphological heterogeneity between individual cells, and a relatively large proportion of cells stained blue can be observed. Quantitative analysis showed that the proportion of SA-β-Gal positive cells was (1.16 ± 0.15)% in CC-P0, which significantly increased to (31.52 ± 3.13)% in CC-P5 (Fig. 1-d). qPCR analysis of the cell cycle arrest gene CDKN1A revealed a higher expression level in CC-P5 compared to CC-P0 (Fig. 1-e). Then we used γH2AX immunofluorescence staining to detect the changes in DNA damage in chondrocytes. In CC-P0, only a few nuclei displayed weak green fluorescence signals, whereas CC-P5 exhibited an increased number of green fluorescence signals, with significant differences in mean fluorescence intensity between the two groups (Fig. 1-f). Decreased proliferative capacity is another critical indicator of

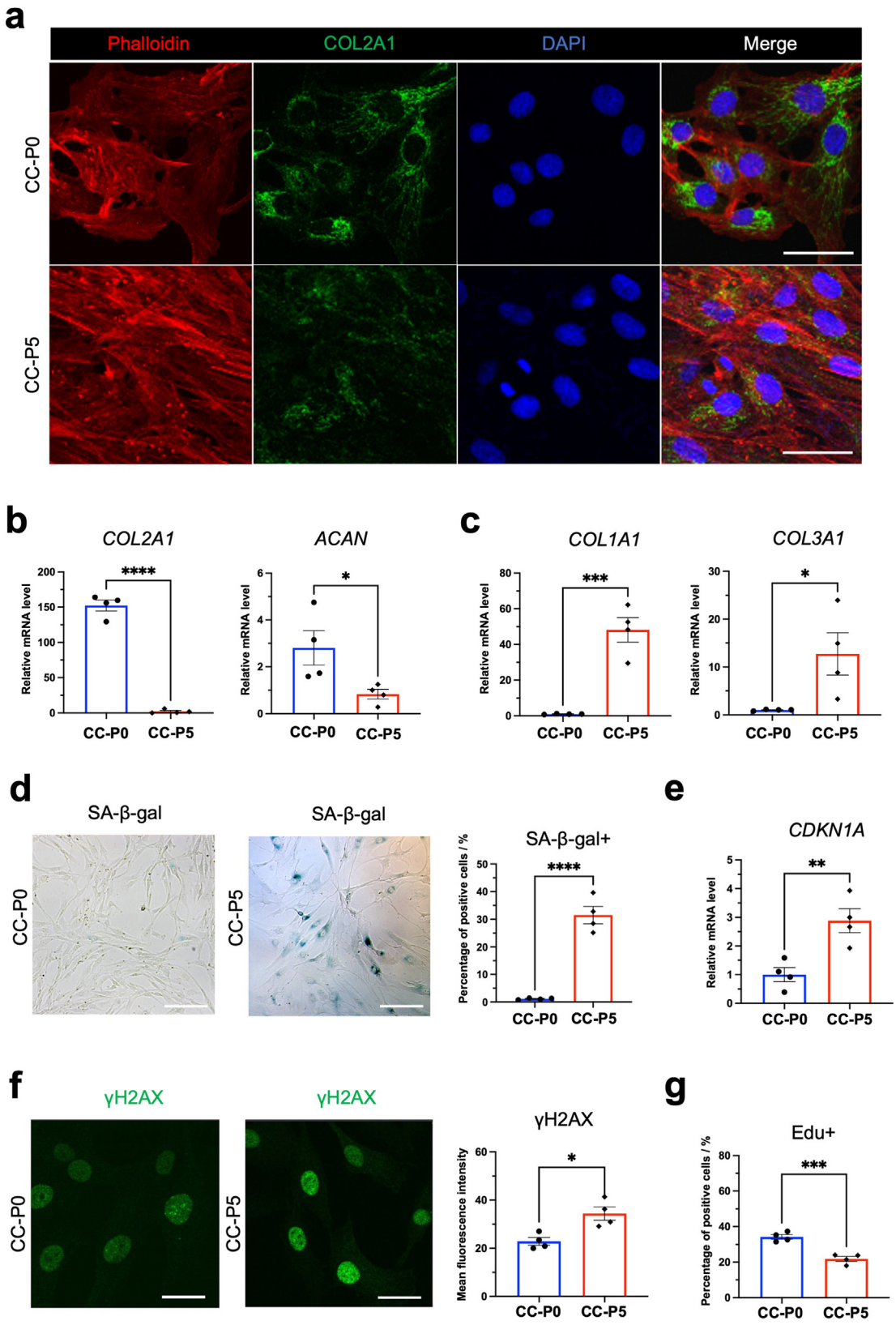

Fig. 1. The senescence of auricular chondrocytes is exacerbated after long-term culture.
(a) Immunofluorescence staining comparing features of CC-P0 and CC-P5. Red denotes positive structures stained with Phalloidin coupled to the 594 fluorophore, while green indicates positive structures stained with COL2A1 primary and CoraLite488 secondary antibodies. Nuclei are stained with DAPI. 200 × magnification; scale bar: 50 μm. (b) qPCR analysis comparing mRNA expression levels of chondrogenic markers COL2A1 and ACAN between CC-P0 and CC-P5. The expression in CC-P5 is set to 1, with CC-P0 expression represented as a multiple of CC-P5. (c) qPCR analysis comparing mRNA expression levels of fibrogenic markers COL1A1 and COL3A1 between CC-P0 and CC-P5. The expression in CC-P0 is set to 1, with CC-P5 expression represented as a multiple of CC-P0. (d) SA-β-gal staining in CC-P0 and CC-P5. Cytoplasmic patchy blue signal indicates positive SA-β-gal staining. 100x magnification; scale bar: 100 μm. Positive ratios for both cell groups are calculated and compared. (e) qPCR detection of the cell cycle proliferation arrest gene

cellular senescence. We further labeled proliferating chondrocytes using the EdU fluorescence probe. The flow cytometry analysis showed that the proportion of EdU positive cells decreased from (34.18 ± 1.3)% in CC-P0 to (21.83 ± 1.4)% in CC-P5 (Fig. 1-g). These results collectively confirm that the degree of senescence in CC-P5 is significantly higher than in CC-P0.

3.2. Mitochondrial dysfunction is a potential cause of senescence in cultured chondrocytes

To prevent the senescence of chondrocytes, it is essential to investigate the primary factors causing senescence in auricular chondrocytes during long-term culture. We conducted transcriptomic sequencing analysis on CC-P0 and CC-P5. Principal component analysis revealed a clear distinction between the two groups (Fig. 2-a). We identified a total of 573 differentially expressed genes (DEGs), with 288 genes upregulated and 285 downregulated in CC-P5 (Fig. 2-b). Gene Ontology (GO) analysis of these DEGs indicated that the upregulated genes were enriched in biological process terms such as cellular response to oxygen-containing compounds, DNA damage response, tissue remodeling, cellular response to cAMP, and response to oxidative stress (Fig. 2-c). Downregulated genes were enriched in terms such as base-excision repair, mitochondrial DNA replication, NADH metabolic process, mitochondrial cytochrome *c* oxidase assembly, and mitochondrial membrane organization (Fig. 2-d). These findings suggest that compared to CC-P0, CC-P5 exhibits more significant oxidative stress damage and mitochondrial dysfunction, the latter being a major cause of oxidative stress and cellular senescence.

We hypothesized that mitochondrial function in auricular chondrocytes progressively deteriorates during long-term in vitro culture. Previous studies have shown that chondrocytes in vitro experience irreversible loss of chondrogenic capacity after two passages. Therefore, we analyzed the mitochondrial structural features of CC-P2 and CC-P5 using transmission electron microscopy. The results showed that mitochondria in CC-P2 commonly possessed recognizable inner membrane cristae, whereas the majority of mitochondria in CC-P5 lacked such structures (Fig. 2-e). We defined mitochondria with ruptured outer membranes and missing inner membrane cristae as irreversibly damaged. Statistical analysis revealed that the proportion of damaged mitochondria increased from (32.67 ± 3.76)% in CC-P2 to (71 ± 4.16)% in CC-P5 (Fig. 2-f). Furthermore, CC-P2 contained abundant autophagosomes engulfing damaged mitochondria, whereas CC-P5 showed fewer autophagosomes (Fig. 2-e). We used the ratio of autophagosomes to damaged mitochondria (A/DM) as an indicator of the cell's ability to clear damaged mitochondria. The analysis showed an A/DM ratio of 1.95 ± 0.11 in CC-P2, which significantly declined to 0.52 ± 0.11 in CC-P5 (Fig. 2-g). These results indicate a correlation between increased retention of damaged mitochondria in the cytoplasm and intensified senescence in CC-P5, suggesting that interventions to reduce mitochondrial oxidative stress damage might alleviate the senescence of auricular chondrocytes during long-term in vitro culture.

3.3. Quercetin alleviates auricular chondrocyte senescence and mitochondrial dysfunction

Based on the previous results, quercetin was selected for its potential to prevent senescence in auricular chondrocytes. We added varying concentrations of quercetin to the culture medium and conducted SA-β-Gal staining in CC-P2 (Fig. 3-a). The results showed that the proportions of SA-β-Gal-positive cells in the 2.5 μM, 5 μM, 10 μM, and 20 μM quercetin groups were (10.03 ± 0.65)%, (6.03 ± 0.31)%, (6 ± 0.34)%, and (7.65 ± 0.49)% respectively, all lower than the control group at (12.45 ± 0.4)%, indicating that quercetin at these concentrations suppressed cellular senescence, with no significant differences observed between the 5 μM, 10 μM, and 20 μM groups (Fig. 3-b). To assess the impact of quercetin on chondrocyte proliferation, we performed a CCK-8 assay. OD_{450nm} value analysis for day 7 cells revealed no significant difference between the 2.5 μM and 5 μM groups, but a gradient decrease in OD_{450nm} values was observed in the 10 μM and 20 μM groups (Fig. 3-c).

From these results, we determined that 5 μM quercetin is the optimal concentration for preventing senescence in cultured chondrocytes. Observations under an phase-contrast microscope showed that cells in the Que (5 μM) group exhibited uniformity and growth as regular spindle shapes, markedly distinct from the control group (Fig. 3-d). To analyze the improvement in mitochondrial function by quercetin, we used the JC-1 fluorescent probe and fluorescence microscopy. Results demonstrated that in the control group, some cells had strong green fluorescence with very weak red fluorescence, indicating severe mitochondrial dysfunction in cells negative for red and positive for green fluorescence (Fig. 3-e). Statistical analysis showed that the proportion of cells with severe mitochondrial dysfunction in the control group was (14.67 ± 1.38)%, which decreased to (7.04 ± 0.36)% in the Que(5 μM) group (Fig. 3-f). Flow cytometry assessing mitochondrial superoxide levels indicated a decrease in MitoSOX fluorescent signal intensity after treatment with Que(5 μM) (Fig. 3-g). Collectively, these results confirm that quercetin alleviates mitochondrial dysfunction and cellular senescence in CC-P2.

3.4. Quercetin improves various functions of mitochondria in auricular chondrocytes

To comprehensively evaluate the effects of quercetin on cellular function, we performed proteomic sequencing analysis on CC-P2. The number of identified proteins in the control group samples was 3852, 4003, and 3652, while in the Que(5 μM) group samples 3990, 4210, and 4014 proteins were identified. Analysis revealed 96 differentially expressed proteins, with 80 upregulated and 16 downregulated in the Que(5 μM) group. For these differentially expressed genes, we conducted GO functional enrichment analysis and KEGG pathway analysis. The results showed that the genes upregulated in the Que(5 μM) group were enriched in biological processes such as DNA-templated transcription, elongation, endoplasmic reticulum tubular network organization, and fatty acid beta-oxidation using acyl-CoA oxidase (Fig. 4-a). KEGG analysis indicated activation of pathways like unsaturated fatty acid biosynthesis and calcium ion reabsorption (Fig. 4-b). The downregulated genes in the Que(5 μM) group were enriched in biological processes such as positive regulation of anoikis and reticulophagy (Fig. 4-c); KEGG analysis showed inhibition of pathways related to proteolytic enzymes and viral life cycle (Fig. 4-d).

To further analyze the specific impact of quercetin on mitochondrial function in auricular chondrocytes, we identified 19 mitochondrial function-related differentially expressed genes, 18 of which were upregulated including DLD, ECI2, HAGH, ACAD9, and

CDKN1A in CC-P0 and CC-P5. The expression in CC-P0 is set to 1, with CC-P5 expression represented as a multiple of CC-P0. (f) Immunofluorescence staining of γH2AX expression in CC-P0 and CC-P5. Green denotes positive structures stained with γH2AX primary and CoraLite488 secondary antibodies. 400 × magnification; scale bar: 10 μm. (g) Statistical analysis of Edu fluorescent probe staining and flow cytometry results in CC-P0 and CC-P5. All experiments utilized cells from auricular samples of four different individuals (n = 4). *p < 0.05, **p < 0.01, ***p < 0.001, ****p < 0.0001.

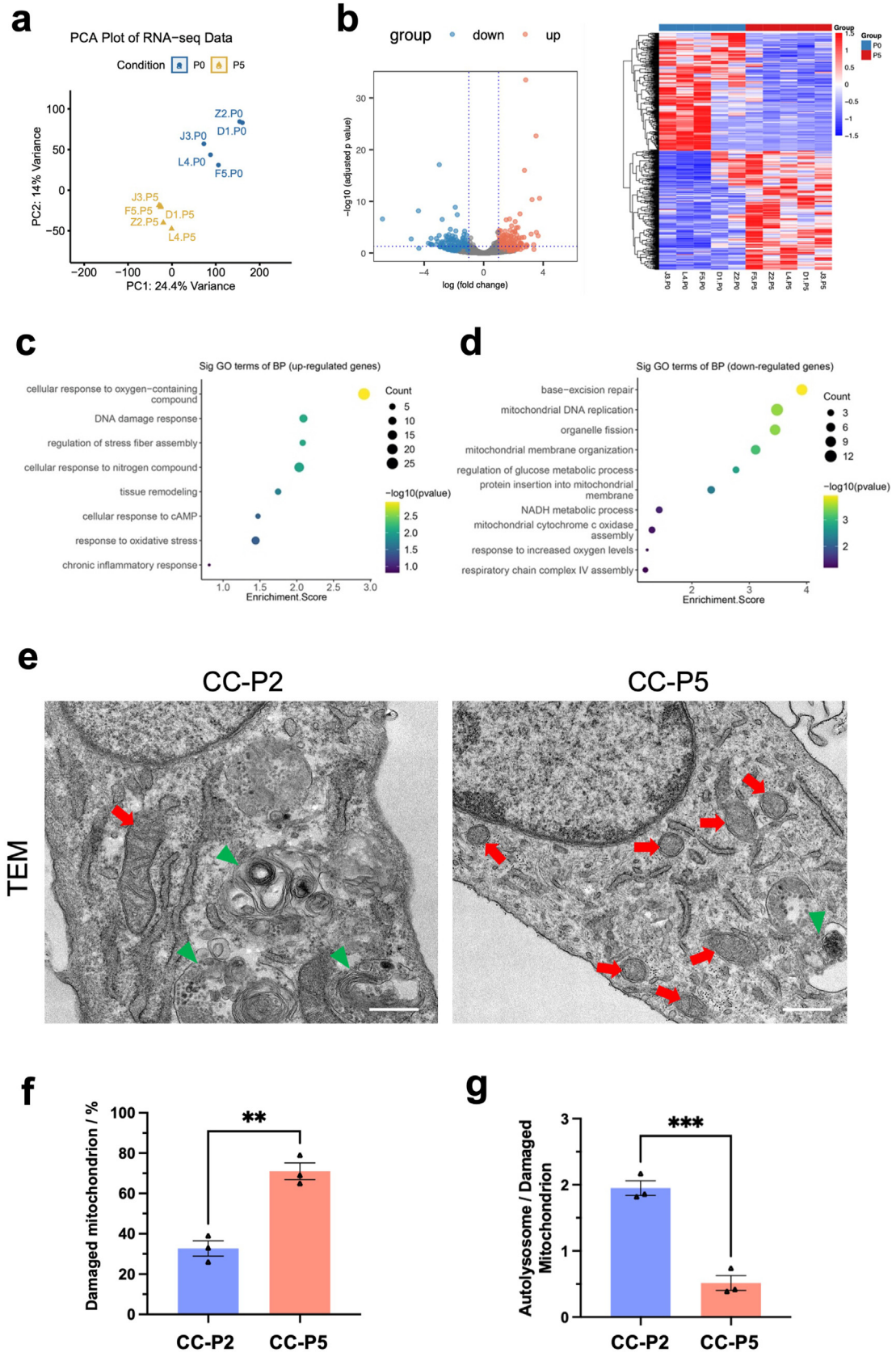

Fig. 2. Mitochondrial dysfunction is a potential cause of senescence in cultured chondrocytes.
(a) Principal component analysis of transcriptome sequencing results from CC-P0 and CC-P5. Cell samples were derived from five cases of auricular cartilage tissue (n = 5). (b) Volcano plot and heatmap depicting differentially expressed genes (DEGs) between CC-P0 and CC-P5. CC-P0 is used as the control group, with blue representing downregulated genes and red representing upregulated genes in CC-P5. DEGs were identified based on an adjusted p-value <0.05 and |log2FC| > 1. (c) Select biological processes (BP) from GO

others, while MRPL24 was downregulated. GO analysis indicated that the upregulated genes were primarily associated with biological processes such as aerobic respiration, cellular respiration, sulfur compound metabolic process, and energy derivation by oxidation of organic compounds (Fig. 4-e). No enriched GO terms were found for the downregulated genes. GSVA analysis of the sequencing data identified 27 mitochondrial function-related pathways with differential enrichment; 24 pathways were upregulated in the Que (5 μM) group, such as Vitamin B2 metabolism, Glycine cleavage system, TIM23 presequence pathway, Fission, and mtDNA nucleoid maintenance; 3 pathways were downregulated, including Cholesterol-associated, Coenzyme A metabolism, and Oxidative phosphorylation assembly (Fig. 4-f). These findings suggest that quercetin possibly mitigates mitochondrial dysfunction through multiple mechanisms, including enhancing electron transport chain activity, metabolic capabilities, and mitochondrial fission, thereby suppressing chondrocyte senescence.

3.5. Quercetin enhances the cartilage regeneration quality of long-term cultured auricular chondrocytes

The aforementioned results suggest that quercetin alleviates mitochondrial dysfunction in CC-P2. We subsequently investigated whether continuous quercetin administration during long-term culture (from CC-P2 to CC-P5) could effectively reduce cellular senescence and preserve chondrogenic capacity. We performed quantitative analysis of senescent cell proportions in CC-P5 using SPiDER-βGal staining and flow cytometry. Results indicated that the proportion of SPiDER-βGal positive cells in the Que(5 μM) group was (24.15 ± 2.66)%, lower than the control group at (31.03 ± 2.1)% (Fig. 5-a).

To assess quercetin's impact on the chondrogenic capacity of long-term cultured auricular chondrocytes, we conducted in vitro three-dimensional chondrogenic induction culture of CC-P5. After 3 weeks of culture, both the control and Que(5 μM) groups formed cartilage pellets in vitro. Macroscopically, pellets in the control group appeared irregular, while those in the Que(5 μM) group were more uniformly spherical. HE staining of tissue sections showed higher cell density and more regular nuclear morphology in the Que(5 μM) group, whereas lower cellular density and more varied nuclear morphology were observed in the control group. Alcian blue staining indicated uniform distribution of blue cartilage extracellular matrix and numerous typical chondrocyte lacunae (red arrows) in the Que(5 μM) group. Immunohistochemical staining confirmed type II collagen expression in both groups, with a higher expression in the Que(5 μM) group (Fig. 5-b).

Finally, we evaluated the effect of quercetin on preventing loss of chondrogenic capacity of long-term cultured auricular chondrocytes through in vivo cartilage regeneration experiments. Results showed both control and Que(5 μM) group CC-P5 formed oval, resilient regenerated cartilage nodules. HE staining of sections revealed better cartilage structure maintenance in the Que(5 μM) group, while irregular morphology and abundant inflammatory cell accumulation were observed at the edges of regenerated cartilage in the control group (Fig. 5-c). Alcian blue staining analysis showed the acidic extracellular matrix content percentage in the Que(5 μM) group was (51.94 ± 6.66)%, significantly higher than the control group's (17.2 ± 3.54)% (Fig. 5-d). Type II collagen immunohistochemistry indicated a higher proportion of positive expression cells in the Que(5 μM) group at (63.47 ± 7.53)%, compared to the control group's (13.83 ± 5.33)% (Fig. 5-e). These comprehensive results demonstrate that Que(5 μM) group CC-P5 exhibit superior chondrogenic capacity.

4. Discussion

Chondrocytes retain adequate chondrogenic functionality during early in vitro expansion (within two passages), but they significantly lose this capacity during later expansion stages (three passages or more). This results in poor-quality regenerated cartilage tissue formation post-implantation [16,17]. This issue poses a significant technical challenge for the tissue-engineered cartilage. Although cellular senescence during in vitro culture has been observed in the field of tissue engineering, the understanding of this phenomenon is not profound, and studies exploring interventions from the perspective of cellular senescence are scarce. Our study comprehensively describes the senescence characteristics of auricular chondrocytes after long-term culture, providing a new perspective to understand the dedifferentiation phenomenon of chondrocytes.

Various external stimuli, such as oxygen tension [18]、nutrient [19]、and substrate stiffness [20], can be sensed by cells, influencing their fate. Sub-lethal damaging stimuli may induce cellular senescence [21]. Senescent cells exist during human development and tissue repair, playing indispensable roles [22,23]. Current arthritis pathogenesis research confirms that increased cellular senescence is a vital cause of irreversible loss of joint cartilage function [24]. Thus, reducing senescent cells can effectively restore the function of chondrocytes in arthritis models [25]. Our study identifies an increase in senescent cells in passaged auricular chondrocytes and explores the factors inducing senescence. From a translational perspective, reducing the proportion of senescent cells during in vitro culture offers a promising strategy to enhance the performance of tissue-engineered cartilage.

This study demonstrated the anti-senescence effects of quercetin from the perspective of changes in the proportion of senescent cells but did not perform an assessment of the senescence-associated secretory phenotype (SASP). Deeply senescent cells secrete various proinflammatory factors, chemokines, growth factors, proteinases, and reactive oxygen species, which can induce the abnormal differentiation or secondary senescence of surrounding healthy cells [26]. Although the composition of the SASP varies across different cell types and senescence-inducing stimuli, it has been widely observed that proinflammatory cytokines, such as interleukin-6 (IL-6), interleukin-8 (IL-8), and monocyte chemoattractant protein-1 (MCP1), are upregulated in all types of senescent cells generated in vitro [27]. Furthermore, the SASP also includes enzymes involved in extracellular matrix (ECM) remodeling, such as matrix metalloproteinases (MMPs), serine/cysteine protease inhibitors (SERPINs), and tissue inhibitors of metalloproteinases (TIMs). Therefore, we speculate that the SASP might be a key mechanism mediating the fibrotic transition of chondrocytes. In this study, we did not assess the SASP in CC-P5 treated with quercetin, and thus, it remains unclear which specific changes in SASP component expression occurred after quercetin treatment in auricular chondrocytes. In future studies, we plan to conduct a comprehensive analysis of the composition and expression levels of the SASP in auricular chondrocytes, which will help to further elucidate the mechanisms by which quercetin suppresses

functional enrichment analysis of upregulated genes (p-value <0.05). (d) Select biological processes (BP) from GO functional enrichment analysis of downregulated genes (p-value <0.05). (e) Transmission Electron Microscopy (TEM) observation of mitochondrial structural characteristics in CC-P2 and CC-P5. Red arrows indicate mitochondria, and green arrows point to autophagolysosomes engulfing damaged mitochondria. 13500 × magnification; scale bar: 0.5 μm. (f) and (g) Statistical analysis of ratios among damaged mitochondria, autophagolysosomes, and injured mitochondria in CC-P2 and CC-P5. Cell samples were derived from three cases of auricular cartilage tissue (n = 3). **p < 0.01, ***p < 0.001.

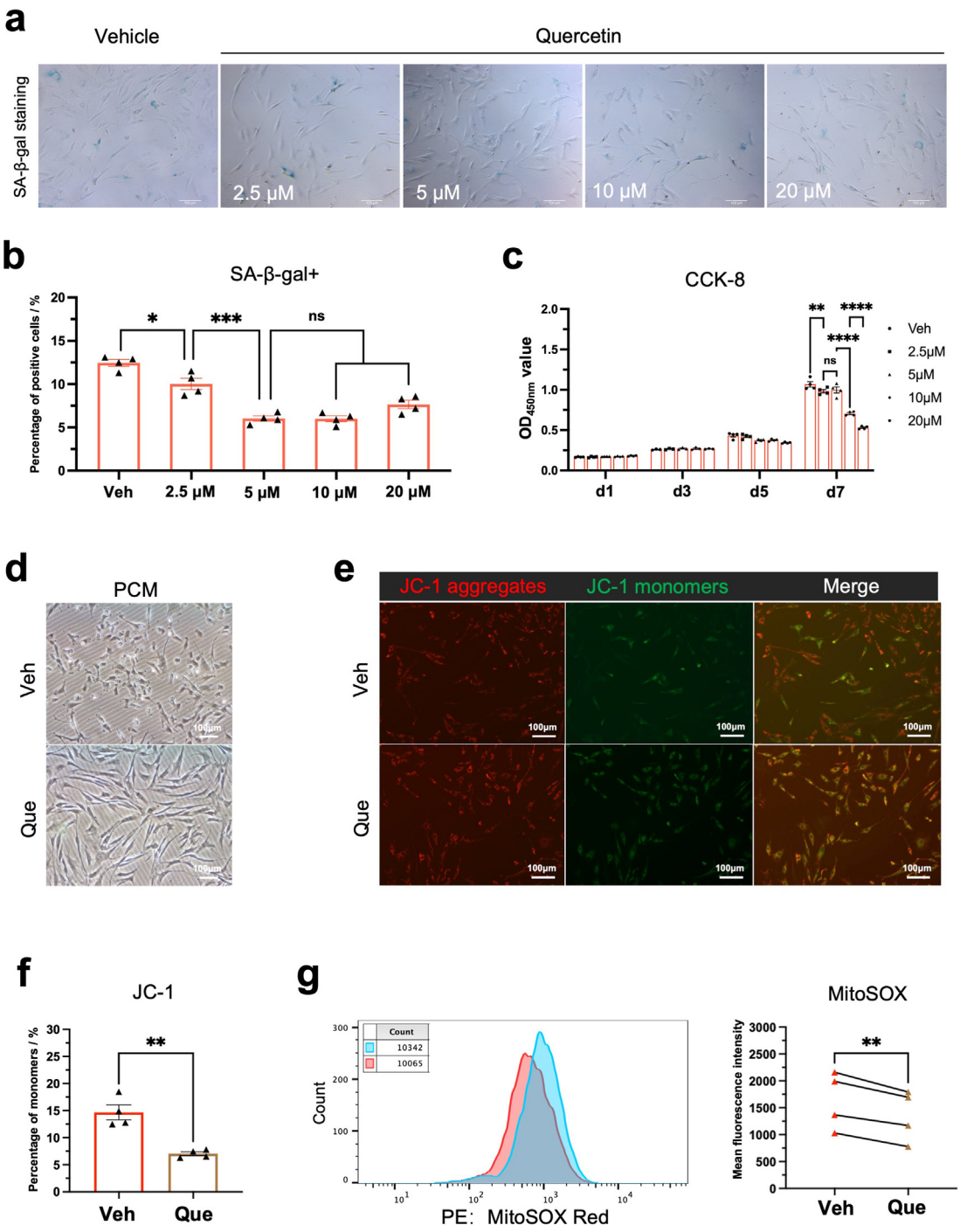

Fig. 3. Quercetin alleviates the senescence of auricular chondrocytes and mitochondrial dysfunction.
(a) SA-β-Gal staining to assess the impact of different quercetin concentrations on the proportion of senescent cells in CC-P2. Patchy blue signals in the cytoplasmic region surrounding the nucleus indicate positive SA-β-Gal staining. 100 × magnification; scale bar: 100 μm. (b) Statistical analysis of the inhibition of CC-P2 cellular senescence by various concentrations of quercetin. (c) CCK-8 assay determining the effect of different quercetin concentrations on CC-P2 cell proliferation. (d) Observation of quercetin's influence on CC-P2 cell growth under an inverted phase contrast microscope. Veh: Vehicle. Que: Quercetin. PCM: Phase Contrast Microscopy. 100 × magnification; scale bar: 100 μm. (e) JC-1 staining to evaluate the impact of Que (5 μM) on mitochondrial membrane potential in CC-P2 cells. Red fluorescence indicates the JC-1 aggregate signal, while green fluorescence denotes the JC-1 monomer signal. 100 × magnification; scale bar: 100 μm. (f) Analysis of JC-1 staining results, comparing cells negative for red fluorescence but positive for green fluorescence. (g) Flow cytometry analysis of quercetin's effect on MitoSOX levels in CC-P2 cells. Average fluorescence intensity of both cell groups is calculated and compared. Cell samples were derived from four cases of auricular cartilage tissue (n = 4). *p < 0.05, **p < 0.01, ***p < 0.001, ****p < 0.0001.

senescence in long-term passaged auricular chondrocytes and enhances cartilage formation quality.

Chondrocytes grown in vivo reside in relatively hypoxic environments, and the oxygen tension levels significantly differ from those in vitro. Cells adapt to environmental changes through compensatory alterations in their cytoskeleton, mitochondria, endoplasmic reticulum, and epigenetic genomic modifications [10,28]. Culturing under physiological oxygen levels (5 %) promotes

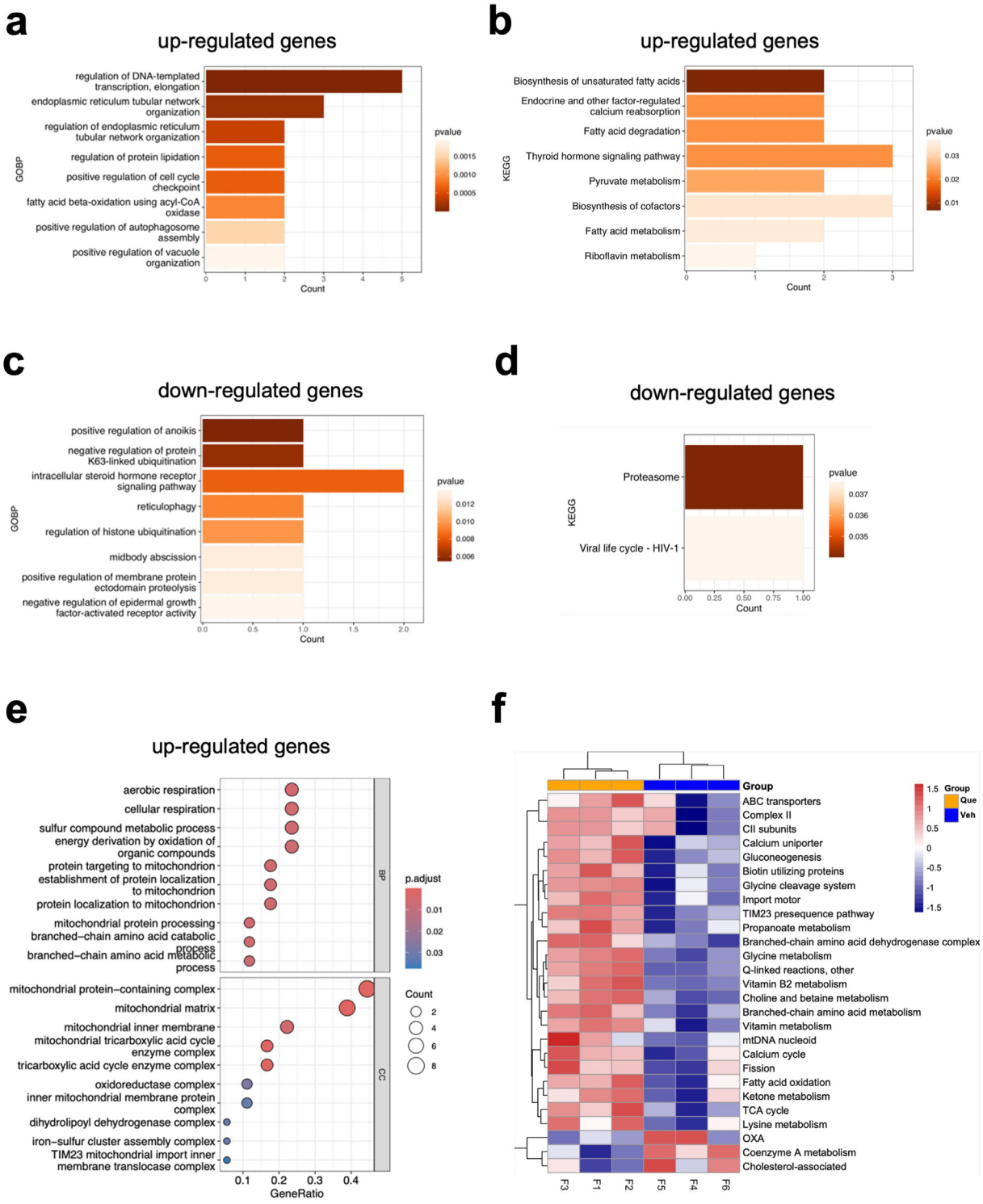

Fig. 4. Quercetin improves various functions of mitochondria in auricular chondrocytes.
(a) GO-BP functional enrichment analysis entries for highly expressed genes in the Que group. (b) KEGG analysis results for highly expressed genes in the Que group. (c) GO-BP functional enrichment analysis entries for lowly expressed genes in the Que group. (d) KEGG analysis results for lowly expressed genes in the Que group. (e) GO-BP and CC analysis entries for highly expressed genes related to mitochondrial function. (f) Gene set variation analysis of differentially expressed genes associated with mitochondrial function.

extracellular matrix deposition in chondrocytes and achieves regenerated cartilage tissue with higher mechanical strength [29]. However, cell proliferation under these conditions is slow, hindering cell expansion. Finding effective strategies to maintain chondrocyte proliferation and inhibit senescence under normoxic conditions is one of the current breakthroughs. Our transcriptomic sequencing revealed mitochondrial dysfunction as a crucial feature of auricular cartilage cellular senescence and chondrogenic capacity loss during in vitro passaging, confirmed by transmission electron microscopy observations.

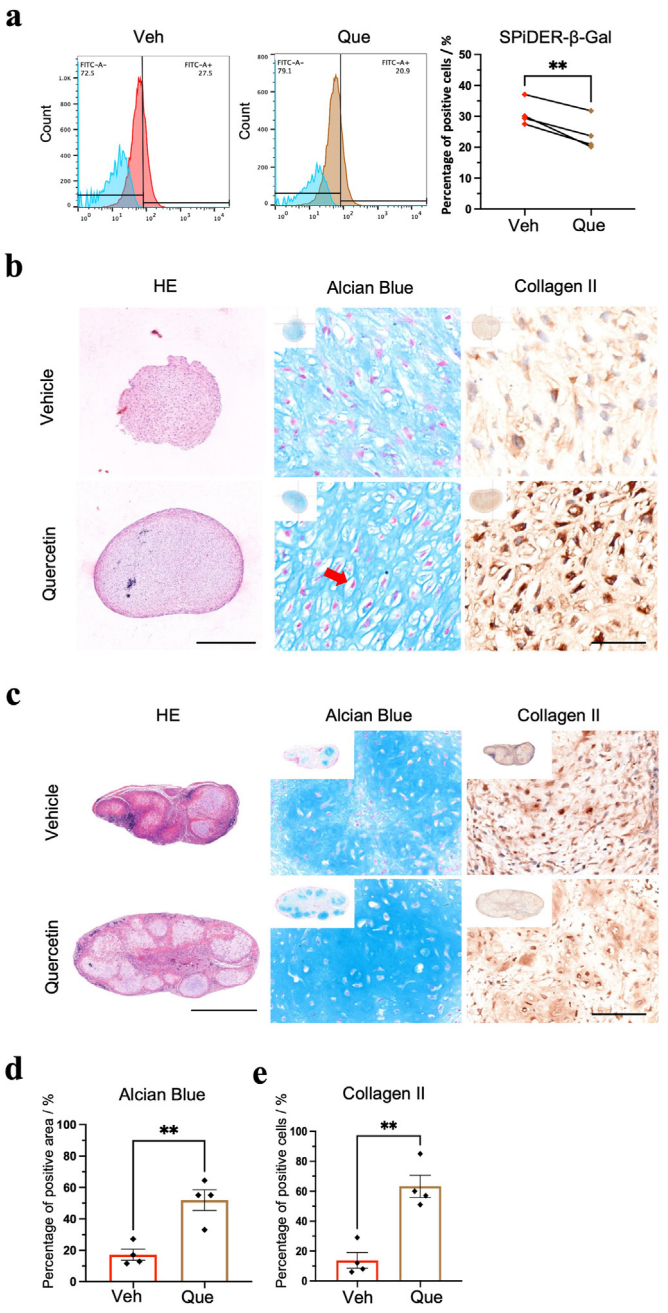

Fig. 5. Quercetin enhances the cartilage regeneration quality of long-term cultured auricular chondrocytes.
(a) The SPiDER-βGal fluorescent probe and flow cytometry were used to assess the proportion of senescent cells in CC-P5. A paired *t*-test was applied for comparison between the control group and the Que (5 μM) group. (b) Three weeks after in vitro three-dimensional chondrogenic induction culture, the CC-P5 from the control and Que (5 μM) groups were subjected to HE staining (2 × magnification; scale bar: 500 μm), Alcian blue staining, and type II collagen immunohistochemical analysis (400 × magnification; scale bar: 50 μm). (c) Upon five weeks of subcutaneous culture in nude mice using GelMA hydrogel-loaded CC-P5 from control and Que (5 μM) groups, the samples were analyzed via HE staining (2 × magnification; scale bar: 500 μm), Alcian blue staining, and type II collagen immunohistochemical detection (200 × magnification; scale bar: 100 μm). (d) Comparison of the positive area of Alcian blue staining between the two groups. (e) Comparison of the proportion of positive cells in immunohistochemical staining between the two groups. All cell samples were drawn from four cases of auricular cartilage tissue (n = 4). **p < 0.01.

Mitochondria function as the primary sites for oxidative metabolism of glucose, lipids, and amino acids within cells. The mitochondrial quality control system dynamically maintains mitochondrial health and homeostasis through processes such as fusion, fission, autophagy, membrane potential regulation, and oxidative phosphorylation. Mitochondria adapt their shape and size to cellular needs through continuous fusion and division while ensuring their pool is replenished by synthesizing new mitochondria to maintain sufficient supply. Autophagic mechanisms are activated to clear damaged mitochondria, preventing accumulation and severe cellular issues.

Chondrocytes transition from glycolytic metabolism in physiological environments to oxidative phosphorylation in vitro, leading to increased mitochondrial number and oxidative phosphorylation activity. High sustained oxidative metabolism elevates mitochondrial radical leakage. Our study confirms increased superoxide content in mitochondria of CC-P5. Cytosolic radicals cause extensive oxidative damage, impairing mitochondrial autophagy and allowing the accumulation of damaged mitochondria [30]. Severely damaged mitochondria experience inner and outer membrane rupture, releasing mtDNA into the cytosol and inducing inflammation and senescence via the cGAS-STING signaling pathway [31]. Our study finds that at the P2 stage, mitochondrial and autophagosome levels remain high, but at P5, there is a notable increase in damaged mitochondria and a decrease in autophagosomes. These results help further understand the issue of dedifferentiation during passaging in auricular chondrocytes, specifically the shift in chondrogenic capacity from reversible to irreversible loss.

Identifying effective methods to mitigate mitochondrial dysfunction in chondrocytes is a crucial area for exploration. Oxidative phosphorylation is a primary mitochondrial function, and restoring the electron transport chain and H^+ flux homeostasis is a fundamental approach. Recent studies on murine chondrocytes reveal that the small molecule BTB06584, which inhibits mitochondrial inner membrane H^+ influx, improves mitochondrial dysfunction in early passage chondrocytes. However, it fails to restore mitochondrial function in late passage [32]. This may be due to the accumulation of severely damaged mitochondria in late passage chondrocytes, which cannot be cleared by autophagy or restored by small molecules, requiring other methods to address mitochondrial dysfunction effectively.

Quercetin's potent antioxidant capability and its safety in human use are well-documented [33]. Its chemical structure, with three aromatic rings and five hydroxyl groups, provides amphipathic properties, facilitating accumulation in membrane organelles like mitochondria and the endoplasmic reticulum. Quercetin at mitochondrial inner membranes captures electron transport chain radicals, reducing oxidative phosphorylation and reactive oxygen production [34]. Hence, quercetin mitigates oxidative damage to mitochondria and other membrane organelles via its strong antioxidant effects. However, high quercetin concentrations significantly restrict oxidative phosphorylation activity and ATP production, causing cytotoxicity. Each cell type and culture condition requires precise determination of efficacious quercetin concentrations. Our study utilized a low concentration of 5 μM to ameliorate mitochondrial dysfunction in chondrocytes, yielding substantial mitochondrial protection and inhibition of senescence. Once cellular senescence has occurred, it signifies that critical structures within the cells, such as mitochondria and DNA, have already incurred significant damage. From an antioxidant perspective, applying quercetin at this stage is no longer within the

optimal time frame to exert its anti-senescence effects, making it challenging to reverse senescent cells to a rejuvenated state. This rationale underlies our decision in this study to administer quercetin during the early passage stage (CC–P2) rather than the late passage stage (CC–P5), where senescent cells had already accumulated substantially.

In this study, we specifically observed and validated the inhibitory effects of quercetin on chondrocyte senescence but did not assess its impact on other cell types. However, numerous recent studies have demonstrated that quercetin exhibits anti-senescence properties across various cell types, including dermal fibroblasts [35], alveolar epithelial cells [36], and adipocytes [37]. Based on these findings, we suggest that the anti-senescence effects of quercetin are not restricted to cartilage-specific changes.

Cellular senescence encompasses multiple levels, including increased senescence degree, augmented senescent cell numbers, reduced stemness of stem/progenitor cells, decreased numbers of stem/progenitor cells, and abnormal differentiation of stem/progenitor cells [38]. Current research indicates that primary chondrocytes extracted from digested cartilage tissue contain both chondroprogenitors with stem traits and mature chondrocytes prone to senescence [39,40].

This study confirms that low-dose quercetin markedly enhances auricular cartilage cell passaging quality and chondrogenic capacity, both in vitro and subcutaneously in nude mice. However, the cartilage samples from microtia patients were collected from both male and female individuals. No stratification by gender was implemented, which may contribute to the limitations of the study's conclusions.

5. Conclusion

Our findings suggest that quercetin attenuates chondrocyte senescence by alleviating mitochondrial dysfunction, thereby preventing the loss of chondrogenic function in chondrocytes subjected to long-term expansion culture.

Ethics approval and consent to participate

This study was approved by the Ethics Committee of the Eye & ENT Hospital of Fudan University (No. 2020069). Informed consent was obtained from the patients before acquiring samples.

Data availability statement

All datasets produced and examined in this study are contained within this article. Additional data can be obtained from the corresponding author upon reasonable request.

Declaration of generative AI and AI-assisted technologies in the writing process

During the preparation of this work the author used GPT-4 in order to improve language and readability. After using this tool, the author reviewed and edited the content as needed and takes full responsibility for the content of the publication.

Funding

This study was funded by the National Natural Science Foundation of China (82371173) and Shanghai Science and Technology Innovation Action Plan (23Y21900200, 21DZ2200700).

Declaration of competing interest

The authors declare that they have no known competing financial interests or personal relationships that could have appeared to influence the work reported in this paper. All authors guarantee the originality of the study and ensure that it has not been published previously. All the listed authors have read and approved the submitted manuscript.

References

[1] Zylinska B, Silmanowicz P, Sobczynska-Rak A, Jarosz L, Szponder T. Treatment of articular cartilage defects: focus on tissue engineering. In Vivo 2018;32(6):1289–300.
[2] Zhou G, Jiang H, Yin Z, Liu Y, Zhang Q, Zhang C, et al. In vitro regeneration of patient-specific ear-shaped cartilage and its first clinical application for auricular reconstruction. EBioMedicine 2018;28:287–302.
[3] Hua Y, Xia H, Jia L, Zhao J, Zhao D, Yan X, et al. Ultrafast, tough, and adhesive hydrogel based on hybrid photocrosslinking for articular cartilage repair in water-filled arthroscopy. Sci Adv 2021;7(35).
[4] Shen Z, Xia T, Zhao J, Pan S. Current status and future trends of reconstructing a vascularized tissue-engineered trachea. Connect Tissue Res 2023;64(5):428–44.
[5] Demoor M, Ollitrault D, Gomez-Leduc T, Bouyoucef M, Hervieu M, Fabre H, et al. Cartilage tissue engineering: molecular control of chondrocyte differentiation for proper cartilage matrix reconstruction. Biochim Biophys Acta 2014;1840(8):2414–40.
[6] Shin H, Lee MN, Choung JS, Kim S, Choi BH, Noh M, et al. Focal adhesion assembly induces phenotypic changes and dedifferentiation in chondrocytes. J Cell Physiol 2016;231(8):1822–31.
[7] Sliogeryte K, Botto L, Lee DA, Knight MM. Chondrocyte dedifferentiation increases cell stiffness by strengthening membrane-actin adhesion. Osteoarthritis Cartilage 2016;24(5):912–20.
[8] Benya PD, Shaffer JD. Dedifferentiated chondrocytes reexpress the differentiated collagen phenotype when cultured in agarose gels. Cell 1982;30(1):215–24.
[9] Ma B, Leijten JC, Wu L, Kip M, van Blitterswijk CA, Post JN, et al. Gene expression profiling of dedifferentiated human articular chondrocytes in monolayer culture. Osteoarthritis Cartilage 2013;21(4):599–603.
[10] Duan L, Liang Y, Ma B, Wang D, Liu W, Huang J, et al. DNA methylation profiling in chondrocyte dedifferentiation in vitro. J Cell Physiol 2017;232(7):1708–16.
[11] Ma J, Zhang Y, Yan Z, Wu P, Li C, Yang R, et al. Single-cell transcriptomics reveals pathogenic dysregulation of previously unrecognised chondral stem/progenitor cells in children with microtia. Clin Transl Med 2022;12(2):e702.
[12] Varela-Eirin M, Varela-Vazquez A, Guitian-Caamano A, Paino CL, Mato V, Largo R, et al. Targeting of chondrocyte plasticity via connexin43 modulation attenuates cellular senescence and fosters a pro-regenerative environment in osteoarthritis. Cell Death Dis 2018;9(12):1166.
[13] Ashraf S, Cha BH, Kim JS, Ahn J, Han I, Park H, et al. Regulation of senescence associated signaling mechanisms in chondrocytes for cartilage tissue regeneration. Osteoarthritis Cartilage 2016;24(2):196–205.
[14] Bai B, Hou M, Hao J, Liu Y, Ji G, Zhou G. Research progress in seed cells for cartilage tissue engineering. Regen Med 2022;17(9):659–75.
[15] Hou M, Bai B, Tian B, Ci Z, Liu Y, Zhou G, et al. Cartilage regeneration characteristics of human and goat auricular chondrocytes. Front Bioeng Biotechnol 2021;9:766363.
[16] Rakic R, Bourdon B, Hervieu M, Branly T, Legendre F, Saulnier N, et al. RNA interference and BMP-2 stimulation allows equine chondrocytes redifferentiation in 3D-Hypoxia cell culture model: application for matrix-Induced autologous chondrocyte implantation. Int J Mol Sci 2017;18(9).
[17] Costa E, Gonzalez-Garcia C, Gomez Ribelles JL, Salmeron-Sanchez M. Maintenance of chondrocyte phenotype during expansion on PLLA microtopographies. J Tissue Eng 2018;9:2041731418789829.
[18] Chakraborty AA, Laukka T, Myllykoski M, Ringel AE, Booker MA, Tolstorukov MY, et al. Histone demethylase KDM6A directly senses oxygen to control chromatin and cell fate. Science 2019;363(6432):1217–22.
[19] Wu YQ, Zhang CS, Xiong J, Cai DQ, Wang CZ, Wang Y, et al. Low glucose metabolite 3-phosphoglycerate switches PHGDH from serine synthesis to p53 activation to control cell fate. Cell Res 2023;33(11):835–50.
[20] Sun Y, Chen CS, Fu J. Forcing stem cells to behave: a biophysical perspective of the cellular microenvironment. Annu Rev Biophys 2012;41:519–42.
[21] Payea MJ, Anerillas C, Tharakan R, Gorospe M. Translational control during cellular senescence. Mol Cell Biol 2021;41(2).
[22] Munoz-Espin D, Canamero M, Maraver A, Gomez-Lopez G, Contreras J, Murillo-Cuesta S, et al. Programmed cell senescence during mammalian embryonic development. Cell 2013;155(5):1104–18.
[23] Jun JI, Lau LF. The matricellular protein CCN1 induces fibroblast senescence and restricts fibrosis in cutaneous wound healing. Nat Cell Biol 2010;12(7):676–85.
[24] McCulloch K, Litherland GJ, Rai TS. Cellular senescence in osteoarthritis pathology. Aging Cell 2017;16(2):210–8.

[25] Jeon OH, Kim C, Laberge RM, Demaria M, Rathod S, Vasserot AP, et al. Local clearance of senescent cells attenuates the development of post-traumatic osteoarthritis and creates a pro-regenerative environment. Nat Med 2017;23(6):775–81.
[26] Huang W, Hickson LJ, Eirin A, Kirkland JL, Lerman LO. Cellular senescence: the good, the bad and the unknown. Nat Rev Nephrol 2022;18(10):611–27.
[27] Di Micco R, Krizhanovsky V, Baker D, d'Adda di Fagagna F. Cellular senescence in ageing: from mechanisms to therapeutic opportunities. Nat Rev Mol Cell Biol 2021;22(2):75–95.
[28] Parreno J, Raju S, Wu PH, Kandel RA. MRTF-A signaling regulates the acquisition of the contractile phenotype in dedifferentiated chondrocytes. Matrix Biol 2017;62:3–14.
[29] Dennis JE, Whitney GA, Rai J, Fernandes RJ, Kean TJ. Physioxia Stimulates extracellular matrix deposition and increases mechanical properties of human chondrocyte-derived tissue-engineered cartilage. Front Bioeng Biotechnol 2020;8:590743.
[30] Bektas A, Schurman SH, Gonzalez-Freire M, Dunn CA, Singh AK, Macian F, et al. Age-associated changes in human CD4(+) T cells point to mitochondrial dysfunction consequent to impaired autophagy. Aging (Albany NY) 2019;11(21):9234–63.
[31] Li T, Chen ZJ. The cGAS-cGAMP-STING pathway connects DNA damage to inflammation, senescence, and cancer. J Exp Med 2018;215(5):1287–99.
[32] Chen Y, Yu Y, Wen Y, Chen J, Lin J, Sheng Z, et al. A high-resolution route map reveals distinct stages of chondrocyte dedifferentiation for cartilage regeneration. Bone Res 2022;10(1):38.
[33] Pawlikowska-Pawlega B, Gruszecki WI, Misiak L, Paduch R, Piersiak T, Zarzyka B, et al. Modification of membranes by quercetin, a naturally occurring flavonoid, via its incorporation in the polar head group. Biochim Biophys Acta 2007;1768(9):2195–204.
[34] Carrillo-Garmendia A, Madrigal-Perez LA, Regalado-Gonzalez C. The multifaceted role of quercetin derived from its mitochondrial mechanism. Mol Cell Biochem 2024;479(8):1985–97.
[35] Zou Z, Long X, Zhao Q, Zheng Y, Song M, Ma S, et al. A Single-cell transcriptomic Atlas of human Skin aging. Dev Cell 2021;56(3):383–397 e8.
[36] Wu W, Wu X, Qiu L, Wan R, Zhu X, Chen S, et al. Quercetin influences intestinal dysbacteriosis and delays alveolar epithelial cell senescence by regulating PTEN/PI3K/AKT signaling in pulmonary fibrosis. Naunyn-Schmiedeberg's Arch Pharmacol 2024;397(7):4809–22.
[37] Matta L, Breves C, Fonte Boa L, Domingos AE, Faria CC, Souza I, et al. Quercetin improves white adipose tissue redox homeostasis in ovariectomized rats. J Endocrinol 2023;259(2).
[38] Munoz-Espin D, Serrano M. Cellular senescence: from physiology to pathology. Nat Rev Mol Cell Biol 2014;15(7):482–96.
[39] Williams R, Khan IM, Richardson K, Nelson L, McCarthy HE, Analbelsi T, et al. Identification and clonal characterisation of a progenitor cell sub-population in normal human articular cartilage. PLoS One 2010;5(10):e13246.
[40] Wu CL, Dicks A, Steward N, Tang R, Katz DB, Choi YR, et al. Single cell transcriptomic analysis of human pluripotent stem cell chondrogenesis. Nat Commun 2021;12(1):362.